Proceedings of the
2005 IEEE Conference on Control Applications
Toronto, Canada, August 28-31, 2005

Gain Scheduling Control Design of an Erbium-Doped Fibre Amplifier by Pump Compensation

Min Ding and Lacra Pavel

***Abstract*— Channel add or drop in a reconfigurable wavelength-division multiplexed (WDM) transmission network produces undesirable transients in the existing channels due to erbium-doped fibre amplifier's (EDFA's) dynamics. We demonstrate a gain scheduling scheme on a PID controller that minimizes the effect of transients by clamping the total EDFA gain of the signal channels through pump power compensation. The scheduled controller requires only three easily accessible parameters: the total input power, the desired and instantaneous total EDFA gains of the signals. This scheduling scheme can stabilize the output signals from an EDFA in less than 1 ms when there is up to 90% drop in the total input signal power. Simulation results for 10 wavelength-division multiplexed channels transmission are presented to demonstrate the effectiveness of the gain scheduling scheme.**

I. Introduction

Erbium-doped fibre amplifiers (EDFA's) provide low-cost and efficient amplification in wavelength-division multiplexed (WDM) networks. As WDM networks advance from static links toward reconfigurable ones, the issue of channels dropping or adding becomes critical. Signal transients at the instance of adding or dropping are not desirable since they cause bit error and in the worst case, catastrophic semiconductor component failure [1].

Several automatic gain control (AGC) schemes have been proposed to minimize the transients [2]–[7]. For instance, [2], [3] propose to add an idle channel as the saturating control signal; however the extra channel is not economical in signal bandwidth. The majority of the control schemes use pump power compensation by means of either feedback or feed-forward controller or both, and demonstrate successful results [4]–[7]. However, all these controllers are designed to function at a fixed operating condition (i.e. fixed input signal power or gain). Since both the input power and gain are determined dynamically in real-life operation, it is critical to have a controller which can operate in a wide range of input signal power and gain. Such a controller can expand the robustness and functionality of WDM networks. In this paper, we investigate gain scheduling techniques on an electronic pump laser controller so that a wide range of operation is achieved.

This work was supported by National Science and Engineering Research Council Undergraduate Student Research Award.

M. Ding is with the Division of Engineering Science, University of Toronto, Toronto, Ontario, M5S 2E4, Canada min.ding@utoronto.ca

L. Pavel is with the Department of Electrical and Computer Engineering, University of Toronto, Toronto, Ontario, M5S 3G4, Canada pavel@control.toronto.edu

This paper is organized as follows. In the next section, the EDFA specification, design requirement and the time-dependent gain model of the EDFA are summarized. In Section III, a linearized mathematical model is generated. After a detailed analysis is performed on this linear model, the optimal PID controller is developed. Section IV describes the methodology of formulating a global controller based on gain scheduling. Simulation results are presented at the end. Finally, conclusions and future research directions are given in Section V.

II. Plant specification and modeling

The previous section has illustrated the importance of the EDFA control in a wide range of operating conditions. In this section, we specify the plant (EDFA) and identify the design constraints and requirements.

A. Plant specification and design requirements

Without loss of generality, we consider ten wavelength-division multiplexed channels. This is sufficient to show the dynamics of an EDFA after channels dropping and adding. We consider typical parameters as used in industry. The ten channels with equal wavelength spacing of 4 nm are chosen from 1528 nm to 1564 nm. The pump laser with wavelength of 980 nm is used although the pump laser with wavelength of 1480 nm can be used as well. The range of operation to be considered is: -10 dBm to 10 dBm input power per channel and 10 dB to 20 dB total gain.

The objective is to keep the output power of each channel constant and to limit the settling time to less than 1 ms when up to 90% of the input power is dropped or added. The only real-time information available to the controller is the total input and total output powers since they are the typical measurements used in the industry at amplifier sites [4]. It is possible to measure the number of the channels, input and output powers of each channel with a spectral analyzer. However, the response time of a spectral analyzer is much longer than our design requirement and its size and economic cost render its implementation at every stage of the EDFA impossible.

B. Time-dependent model of EDFA

Next, we briefly describe the mathematical model of the plant. There are many existing models describing the EDFA such as steady-state models, transients and dynamic models

0-7803-9354-6/05/$20.00 ©2005 IEEE

and perturbation models [8]. We use the time-dependent gain model from [9] due to its simplicity and wide application. From [9], the average fraction of atoms in the upper energy level along an EDFA, $\overline{N_2}(t)$, the output power of the i^{th} channel, $p_i^{out}(t)$ and the total gain, $G(t)$ are expressed as:

$$
\begin{aligned}
LS\rho(\frac{d}{dt}+\frac{1}{\tau_o})\overline{N_2}(t) &= p_{pump}(t) \\
&\quad -\sum_{i=1}^{N} p_i^{in}(t)\{exp[((\gamma_i+\alpha_i)\overline{N_2}(t)-\alpha_i)L]-1\} \\
p_i^{out}(t) &= p_i^{in}(t)exp[((\gamma_i+\alpha_i)\overline{N_2}(t)-\alpha_i)L] \\
G(t) &= \frac{p_{total}^{out}(t)}{p_{total}^{in}(t)}
\end{aligned}
\tag{1}
$$

where

$$
\begin{aligned}
p_{total}^{in}(t) &= \sum_{i=1}^{N} p_i^{in}(t) \\
p_{total}^{out}(t) &= \sum_{i=1}^{N} p_i^{out}(t)
\end{aligned}
$$

In the foregoing, τ_o is the spontaneous lifetime of the upper energy level; ρ is the density of the active erbium atoms; S is the fibre core cross section area; L is the length of the EDFA; N is the total number of signal channels; $p_i^{in}(t)$ is the input power of the i^{th} channel; $p_{pump}(t)$ is the pump power; α_i and γ_i are the absorption and emission coefficients for the i^{th} signal channel.

III. Linear controller design for the plant

Before designing a controller for a plant, it is not only necessary to understand the dynamics of the plant, but also required to identify all the accessible parameters. In this section, we first identify the appropriate control scheme with the given parameters, then design a controller for the linearized plant.

A. Plant linearization

In the case of EDFA control, we do not have access to all the parameters, such as the average upper level fraction, number of channels, input and output power of each channel as listed in Section II. With this consideration, the controller options are greatly limited; the controller design will be based on the EDFA's input and output, which are measurable in real-time.

The objective of keeping the output power of each channel constant after channels dropping or adding needs to be reformulated, since we cannot access these parameters. We consider the new objective of controlling the EDFA so that the total gain remains constant after channels dropping or adding. Although the total gain is the weighted average of the channel gains, by controlling this value constant, the gain and the output power of each channel should remain approximately constant. Thus, the desired controller needs to receive the total gain as an input and regulate the pump power in order to achieve a constant total gain.

TABLE I

Expressions for the parameters of the linear model of the EDFA

Notation	Expression
A	$-\frac{1}{\tau_o}\{1+\frac{\tau_o}{S\rho}\sum_{i=1}^{N} p_i^{ino}exp[((\gamma_i+\alpha i)\overline{N_2^o}-\alpha_i)L](\gamma_i+\alpha i)\}$
B_1	$B_1(i,1)=\frac{p_i^{ino}-p_i^{outo}}{p_i^{ino}SL\rho}, \forall i=1,2,...,N$
B_2	$\frac{1}{SL\rho}$
C_1	$C_1(1,i)=p_i^{outo}(\gamma_i+\alpha_i)L, \forall i=1,2,...,N$
D_{11}	$D_{11}(i,j)=\begin{cases}\frac{p_i^{outo}}{p_i^{ino}} & \text{i = j} \\ 0 & \text{otherwise}\end{cases} \quad \forall i,j=1,2,...,N$
D_{12}	0
C_2	$\frac{\sum_{i=1}^{N} p_i^{outo}(\gamma_i+\alpha_i)L}{p_{total}^{ino}}$
D_{21}	$D_{21}(1,i)=\frac{exp[((\gamma_i+\alpha i)\overline{N_2^o}-\alpha_i)L]}{p_{total}^{ino}}-\frac{p_{total}^{outo}}{(p_{total}^{ino})^2}, \forall i=1,2,...,N$
D_{22}	0
x	$\overline{N_2}(t)-\overline{N_2^o}$
$P_{in}(t)$	$[p_1^{in}(t)-p_1^{ino}, p_2^{in}(t)-p_2^{ino}, ..., p_N^{in}(t)-p_N^{ino}]^T$
u(t)	$p_{pump}(t)-p_{pump}^o$
$P_{out}(t)$	$[p_1^{out}(t)-p_1^{outo}, p_2^{out}(t)-p_2^{outo}, ..., p_N^{out}(t)-p_N^{outo}]^T$
y(t)	$G(t)-G^o$

With these considerations and based on (1), which describes the nonlinear behavior of the EDFA, a linearized model is generated below at a nominal operating condition ($\overline{N_2^o}$, p_{pump}^o, G^o, p_i^{ino}, and p_i^{outo}, $\forall i=1,2,...,N$). Note that the average upper level fraction is treated as the state vector (x) and the pump power is considered separately from the signal channels. Also, the pump power and the total gain after linearization are treated as the input (u) and the output (y) of the plant, respectively.

$$
\begin{aligned}
\frac{dx(t)}{dt} &= Ax(t)+B_1P_{in}(t)+B_2u(t) \\
P_{out}(t) &= C_1x(t)+D_{11}P_{in}(t)+D_{12}u(t) \\
y(t) &= C_2x(t)+D_{21}P_{in}(t)+D_{22}u(t)
\end{aligned}
\tag{2}
$$

where the expressions for the state-space parameters are summarized on Table I. A conceptual diagram of the linear model of the EDFA from (2) is shown in Fig. 1. It shows that the design objective is to control a single-input-single-output (SISO) plant in order to achieve constant output regulation. Essentially, approximately constant output power of each channel is considered as the byproduct of this total gain regulation. The transfer function of this SISO plant is given as:

$$
G(s)=\frac{B_2C_2}{s-A} \tag{3}
$$

Clearly this is a single pole plant with its pole at A and DC gain of $-\frac{B_2C_2}{A}$.

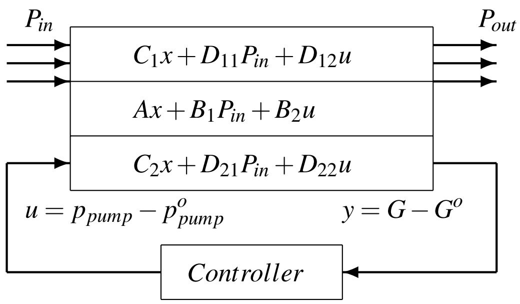

Fig. 1. Conceptual diagram of the linear model of the EDFA with an controller

B. Linear controller design

For simplicity, we can rewrite (3) as:

$$
\begin{aligned}
G(s) &= \frac{K_p}{s+\omega_{OL}} \\
K_p &= \frac{\sum_{i=1}^{N} p_i^{outo}(\gamma_i+\alpha_i)L}{SL\rho p_{total}^{ino}} \\
\omega_{OL} &= \frac{1}{\tau_o}\{1 + \frac{\tau_o}{S\rho}\sum_{i=1}^{N} p_i^{outo}(\gamma_i+\alpha_i)\}
\end{aligned} \quad (4)
$$

where ω_{OL} is the open loop pole and the parameters are as in (1). We shall design a proportional-integral-derivative (PID) controller in cascade form [10], [4]

$$
PID : K_{PID}(s) = K_r \frac{(1+\tau_1 s)(1+\tau_2 s)}{\tau_1 s(1+0.1\tau_2 s)} \quad (5)
$$

which is convenient for frequency domain design and for selection of τ_1 and τ_2. In order to increase the phase margin of the loop-gain function, $G(s)K_{PID}(s)$, from simulations it is found that $\tau_1 = \frac{1}{5\omega_{OL}}$ and $\tau_2 = \frac{3}{50\omega_{OL}}$ are optimal. With the proposed values of τ_1 and τ_2, a minimum phase margin of $50\ ^o$ is ensured.

The next step is to identify the gain, K_r of the controller. Since we have a simple single-pole plant, we can use direct calculation by pole placement [11]. The characteristic equation of the closed loop system is given as:

$$
\tau_1 s(1+0.1\tau_2 s)(s+\omega_{OL}) + K_p K_r (1+\tau_1 s)(1+\tau_2 s) \quad (6)
$$

K_r should be designed so that the closed loop poles are placed in desirable locations. However, since the dynamics changes in different operating conditions, we have to first normalize K_r with respect to the dynamics of the plant. The reason is that one K_r value can be optimal in one operating point but might not be suitable for other points. Therefore, we consider the product K_pK_r as one variable, which is chosen to be proportional to ω_{OL}. By this selection, all the parameters in (6) are normalized to the open loop pole, and thus, pole placement is valid regardless of the operating condition. We rewrite (6) as:

$$
\tau_1 s(1+0.1\tau_2 s)(s+\omega_{OL}) + C\omega_{OL}(1+\tau_1 s)(1+\tau_2 s) \quad (7)
$$

where $C\omega_{OL}$ is the product K_pK_r and C is a constant. After substituting expressions for τ_1 and τ_2 in terms of ω_{OL}, we arrive at the following equation.

$$
s^3 + (\frac{503}{3} + 10C)\omega_{OL}s^2 + (\frac{500+650C}{3})\omega_{OL}^2 s + \frac{2500c}{3}\omega_{OL}^3 \quad (8)
$$

Based on root locus method, we identify the optimal C, which places the closed loop poles at $7.6\omega_{OL}, 7.6\omega_{OL}$, and $491\omega_{OL}$. This configuration of the closed loop poles far away from the origin and without imaginary part, yields a short settling time and minimum overshoot. The parameters of the PID controller are summarized on Table II.

TABLE II
THE PID CONTROLLER'S PARAMETERS

Parameters	K_r	τ_1	τ_2
PID	$\frac{33.8\omega_{OL}}{K_p}$	$\frac{1}{5\omega_{OL}}$	$\frac{3}{50\omega_{OL}}$

C. Simulation with linear plant

After this controller design, the system simulation with the PID controller and the linearized plant is presented next. The inputs are -10 dBm from each of the 10 channels and the total gain is set to be 10 dB. Note that the phase margin and the shape of the graphs should not be input dependent, since our controller is normalized to ω_{OL}. However, the settling time is inversely proportional to ω_{OL}. The diagrams on Fig. 2 include: Bode plot of the loop gain transfer function (GK_{PID}), Bode plot of self-amplification of channel 2, Bode plot of cross-talk between channel 2 and channel 1 and step response of channel 1 with respect to channel 2. Note that the settling time is in order of 0.1 ms (Fig. 2(d)), well within our design requirement. This outcome is for the plant with ω_{OL} at 3227 rad/s. Since the typical total gain of the EDFA is above 10 dB, this can be considered as the worst case with the minimum ω_{OL}. Thus, the settling times of the linearized system are generally less than 0.1 ms.

IV. GAIN SCHEDULING CONTROL OF THE EDFA

Based on the linearized controller in Section III, a gain scheduling control scheme is proposed in this section. Simulation results are presented for the nonlinear model (1) and the gain scheduled controller.

A. Gain scheduling

The EDFA model in (1) is a highly non-linear system. By evaluating the expression of ω_{OL} (4) for typical parameter ranges, it can be shown that ω_{OL} varies from 1000's rad/s to 10000's rad/s. It is obvious that a controller designed for a single operating point is not sufficient to effectively control the EDFA over the entire range of operating conditions.

Among many possible nonlinear control techniques, gain scheduling is explored due to its simplicity and popularity. A classical gain scheduling approach [12] is based on linearizing the nonlinear system at several operating points and designing a linear controller for each operating point

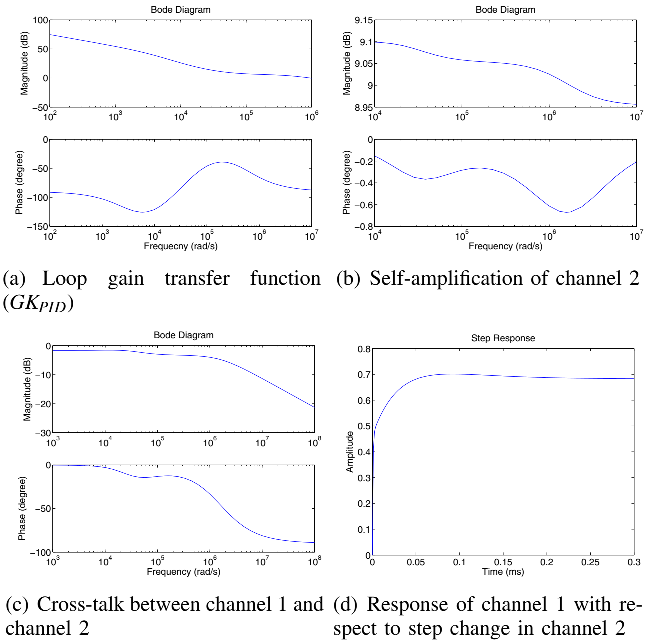

(a) Loop gain transfer function (GK_{PID})

(b) Self-amplification of channel 2

(c) Cross-talk between channel 1 and channel 2

(d) Response of channel 1 with respect to step change in channel 2

Fig. 2. System response with the PID controller and the linearized plant

to achieve satisfactory result. A global nonlinear controller is developed by interpolating, or "scheduling", the linear controllers designed previously.

In fact, all these three steps are completed in the previous section. We have a nonlinear equation (1) which completely describes the dynamics of the plant, and we have derived all the parameters of the controller for any operating condition. Effectively, the number of our operating points for consideration is infinite. This method of incorporating infinite number of operating points by exploiting the advantage of knowing the dynamics of the plant is believed to ensure the perfect selection of the controller at any operating condition. Since we have complete understanding of the plant's dynamics and are able to design a controller at any operating condition, the necessity of interpolation is bypassed.

However, the controller depends on the operating condition of the plant. In order to determine which operating point the plant is at, we consider (4). The plant is represented as a single pole system with its gain and pole as functions of p_i^{ino}, p_i^{outo}, $\forall i = 1,...,N$ and $\overline{N_2^o}$, since the device parameters such as L, S, τ_o, α_i's and γ_i's are known constants. Therefore, in principle, we can find the exact linear system representation (i.e. K_p and ω_{OL}) of the EDFA at any operating point from these parameters. However, none of $p_i^{in}(t)$'s, $p_i^{out}(t)$'s and $\overline{N_2}(t)$ are measurable in real time. To find an accurate estimate of the plant's operating condition, we need to estimate K_p and ω_{OL} from the parameters that can be directly measured, i.e. $p_{total}^{in}(t), p_{total}^{out}(t)$ and G(t). With this consideration, the expressions for K_p and ω_{OL} (4) can be rewritten as,

$$K_p = \frac{\overline{\gamma+\alpha}\rho G^o}{S} \tag{9}$$

$$\omega_{OL} = \frac{1}{\tau_o}\{1 + \frac{\tau_o}{S\rho}\overline{\gamma+\alpha}\, p_{total}^{ino} G^o\} \tag{10}$$

where $G^o = \frac{p_{total}^{outo}}{p_{total}^{ino}}$ as in (1), and $\overline{\gamma+\alpha}$ is the weighted average of N channels' $\gamma+\alpha$ defined as:

$$\overline{\gamma+\alpha} = \sum_{i=1}^{N} \frac{p_i^{outo}}{p_{total}^{outo}}(\gamma_i + \alpha_i) \tag{11}$$

From values of γ and α, we can calculate that $\overline{\gamma+\alpha}$, (11) attains a value from 1.28 to 2.91. We approximate this value by 2.09, the mean of its attainable range. Even though this approximation can result in up to 63% error, the controller designed for the mismatched plant can still yield satisfactory performance. If we compare the two loop gain transfer functions, the difference is found to be insignificant. Furthermore, the mean of the attainable range is a reasonably accurate estimation since the EDFA usually operates with multiple inputs with equal power (in general, the EDFA is followed by dynamic optical filters for equalizing wavelength channels' powers [4]).

From (9) and (10), we can represent the transfer function of the plant by two measurable parameters, $p_{total}^{in}(t)$ and G(t). These two variables are called the scheduling variables since they indicate when and how the controller should be changed. Finally, we can represent the dynamics of the resulting nonlinear controller as:

$$\begin{aligned} \dot{x_c} &= f(x_c(p_{total}^{in}, G), u_c(p_{total}^{in}, G), p_{total}^{in}, G) \\ y_c &= g(x_c(p_{total}^{in}, G), u_c(p_{total}^{in}, G), p_{total}^{in}, G) \end{aligned} \tag{12}$$

where x_c is the state vector of the controller, u_c is $G - G^o$, y_c is $p_{pump} - p_{pump}^o$ and f, g are generic functions representing the dynamics of the controller.

In the rest of the subsection, a theoretical justification is presented to ensure satisfactory performance of this controller. Gain scheduling is a common engineering practice to control nonlinear systems and it has provided numerous successful results [13], [14]. However, it still remains as an ad hoc technique since the performance and the stability of a globally gain scheduled system can not be determined explicitly. Often, these properties are inferred from extensive simulation results [15]. To ensure that a satisfactory performance is maintained over the entire operating conditions, a controller analysis is performed following after [14]. The main idea is to ensure removal of hidden coupling terms due to scheduling variables. Theoretical reasoning for this is given in [12], [16]. In summary, hidden coupling terms are defined as non-zero partial derivatives with respect to the scheduling variables (p_{total}^{in} and G) in (12). These coupling terms prevent the gain scheduled system from behaving in accordance with the linear controller and plant. Thus, it is important to remove them by satisfying the following conditions [14], around any operating point(p^{ino}_{total}, G^o):

$$
\begin{aligned}
\frac{\partial f}{\partial p^{ino}_{total}}(x_c(p^{ino}_{total}, G^o), u_c(p^{ino}_{total}, G^o), p^{ino}_{total}, G^o) = 0\\
\frac{\partial f}{\partial G^o}(x_c(p^{ino}_{total}, G^o), u_c(p^{ino}_{total}, G^o), p^{ino}_{total}, G^o) = 0\\
\frac{\partial g}{\partial p^{ino}_{total}}(x_c(p^{ino}_{total}, G^o), u_c(p^{ino}_{total}, G^o), p^{ino}_{total}, G^o) = 0\\
\frac{\partial g}{\partial G^o}(x_c(p^{ino}_{total}, G^o), u_c(p^{ino}_{total}, G^o), p^{ino}_{total}, G^o) = 0
\end{aligned}
\tag{13}
$$

These conditions can be further specified. Consider the following state matrices derived from linearizing (12),

$$
\begin{aligned}
A_c(p^{ino}_{total}, G^o) &= \frac{\partial f}{\partial x_c}(x_c(p^{ino}_{total}, G^o), u_c(p^{ino}_{total}, G^o), p^{ino}_{total}, G^o)\\
B_c(p^{ino}_{total}, G^o) &= \frac{\partial f}{\partial u_c}(x_c(p^{ino}_{total}, G^o), u_c(p^{ino}_{total}, G^o), p^{ino}_{total}, G^o)\\
C_c(p^{ino}_{total}, G^o) &= \frac{\partial g}{\partial x_c}(x_c(p^{ino}_{total}, G^o), u_c(p^{ino}_{total}, G^o), p^{ino}_{total}, G^o)\\
D_c(p^{ino}_{total}, G^o) &= \frac{\partial g}{\partial u_c}(x_c(p^{ino}_{total}, G^o), u_c(p^{ino}_{total}, G^o), p^{ino}_{total}, G^o)
\end{aligned}
\tag{14}
$$

Thus, differentiating (12) with respect to p^{ino}_{total} and G^o and using (13) and (14) yields a set of equivalent conditions:

$$
\begin{aligned}
&A_c(p^{ino}_{total}, G^o)\left[\ \frac{\partial x_c(p^{ino}_{total}, G^o)}{\partial p^{ino}_{total}} \quad \frac{\partial x_c(p^{ino}_{total}, G^o)}{\partial G^o}\ \right]\\
&\quad + B_c(p^{ino}_{total}, G^o)\left[\ \frac{\partial u_c(p^{ino}_{total}, G^o)}{\partial p^{ino}_{total}} \quad \frac{\partial u_c(p^{ino}_{total}, G^o)}{\partial G^o}\ \right]\\
&\quad = [\ 0 \quad 0\ ]\\
&C_c(p^{ino}_{total}, G^o)\left[\ \frac{\partial x_c(p^{ino}_{total}, G^o)}{\partial p^{ino}_{total}} \quad \frac{\partial x_c(p^{ino}_{total}, G^o)}{\partial G^o}\ \right]\\
&\quad + D_c(p^{ino}_{total}, G^o)\left[\ \frac{\partial u_c(p^{ino}_{total}, G^o)}{\partial p^{ino}_{total}} \quad \frac{\partial u_c(p^{ino}_{total}, G^o)}{\partial G^o}\ \right]\\
&\quad = \left[\ \frac{\partial y_c(p^{ino}_{total}, G^o)}{\partial p^{ino}_{total}} \quad \frac{\partial y_c(p^{ino}_{total}, G^o)}{\partial G^o}\ \right]
\end{aligned}
\tag{15}
$$

Although in general, these conditions require extensive calculation and sometimes cannot be satisfied [14], it can be easily verified that the PID controller considered here meets these conditions. At steady state, $u_c(p^{ino}_{total}, G^o)$ is zero because it is the difference between the actual total gain and the desired total gain. Similarly, $y_c(p^{ino}_{total}, G^o)$ needs to be zero due to the integral action of the PID controller (i.e. pole at s = 0). From $y_c(p^{ino}_{total}, G^o) = C_c(p^{ino}_{total}, G^o)x_c(p^{ino}_{total}, G^o) + D_c(p^{ino}_{total}, G^o)u_c(p^{ino}_{total}, G^o)$, we induce that $x_c(p^{ino}_{total}, G^o)$ is zero at steady state as well, since $C_c(p^{ino}_{total}, G^o)$ is non-zero. Thus, (15) is satisfied for the PID controller. Note that even though (15) appears to be a trivial condition, this is solely due to the integral action which ensures zero output at steady state. The advantageous effect of integral action to achieve local linear equivalence (removal of hidden coupling terms) at equilibrium points has been well documented [17]. Thus, we have ensured the removal of the hidden coupling terms at steady state.

B. Unsuccessful gain scheduling on fast varying values

We tested the nonlinear plant and the gain scheduled PID controller via simulation. Due to fast varying scheduling parameters, the simulation failed. It is often observed [15] that a parameter dependent system is stable with fixed parameter values but loses stability when parameters are time varying. Thus, one of the fundamental gain scheduling guidelines is to schedule controller with slow varying parameters [12]. A theoretical justification for this is given in [15]. The reason is that the controller design is based on a stable plant parameterized by the scheduling variables, while the real plant has not reached its steady state. Therefore, the imaginary plant represented by the scheduling variables does not give an accurate estimate of the real plant and the initially planed performance at steady states can not be expected. Note that the poor performance or the instability of the system is not due to poor stability margin of the system at its steady state. It is rather due to inaccurate representation of the plant.

This situation can be avoided by using scheduling variables with slow variation, which allow accurate representation of the real plant. In the case of EDFA control, the scheduling variables are $p^{in}_{total}(t)$ and $G(t)$. Since $p^{in}_{total}(t)$ is fixed before channels dropping or adding, it is expected that G(t) varies extremely fast. This fast varying $G(t)$ causes the gain scheduled controller to change intensively and results in instability. Due to the design constraints, there are no other possible variables we can measure. The average upper level fraction is the most suitable scheduling variable because it best represents the "physics" of the EDFA and it varies relatively slowly (the spontaneous life time of the upper energy level is 10 ms). However, we cannot access this parameter due to the design constraints set earlier.

C. Scheduling scheme with frozen parameters

As mentioned above, the fast variation of G(t) is the major cause of the instability of the gain scheduled system. The only possible scheduling variable that indicates the nonlinear nature of the EDFA and is accessible and slow varying, is the desired total gain, denoted as $G_{ref}(t)$. Although the desired total gain is an external reference value, and not a direct indicator of the operating condition of the plant, the total gain of the plant is expected to reach this value at steady state, i.e. $G^o = G_{ref}$. Therefore, under the condition of no change in the total input power and the desired total gain, we have a fixed controller which should ensure a stable system near equilibrium points. The problem that naturally arises is how to schedule the controller when there is a change in the input power or in the desired total gain. An instant switch between the controllers might result in poor performance of the system. Therefore, the following scheduling scheme is proposed based on the scheduling variables $p^{in}_{total}(t)$ and $G_{ref}(t)$:

1) Upon detection of any change in $p^{in}_{total}(t)$ or $G_{ref}(t)$ above certain threshold, the gain scheduling starts.

2) Define the steady state before the gain scheduling as the old state and the future steady state the system will eventually reach with the given new $p_{total}^{in}(t)$ and $G_{ref}(t)$ as the new state. The controller designed for the old state will be used for the next 200 μs.
3) After 200 μs, an intermediate controller is created from linearly time-weighted interpolating the τ's and the K_r of the two controllers for the old and new states in the next 800 μs. This is equivalent to (16), where t is the time (in μs) measured 200 μs after the gain scheduling starts.

$$\tau = \frac{t}{800}\tau_{new} + \frac{800-t}{800}\tau_{old}$$
$$K_r = \frac{t}{800}K_{rnew} + \frac{800-t}{800}K_{rold} \quad (16)$$

4) After linearly time-weighted interpolation (i.e. 1 ms after the scheduling starts), the controller for the new state is left to operate till another change is detected.

The decision of 200 μs as the boundary between the old controller and the intermediate controller is based on the simulation results and intuition to the physical nature of the EDFA. In reality, the optimal time interval depends on the average upper level fraction in the old and new states.

The simulation results with the use of the scheduled PID controller are summarized below. The simulation scenario is: the input power is -10 dBm from each of the ten channels and the desired total gain is set to be 20 dB. Five channels are added at 4 ms to the five existing channels and then dropped later at 6 ms. As shown on Fig. 3, the gain scheduling scheme on the PID controller is effective. The total gain is controlled to be at 20 dB with a settling time less than 0.1 ms (Fig. 3(c)). As the result, the output power of each channel remains relatively constant. However, at the instant of channels dropping or adding, a sudden drop or surge occurs in the pump power. Even though the spike lasts for an extremely short period, it still renders the controller impossible to be implemented. As shown on Fig. 3(b), the spike rises up to 2 W during channels adding and drops to -4 W during channels dropping. Obviously, it is infeasible to output a negative pump power. Also, there is a limitation on the maximum pump power that can be produced by a laser. Thus, as one of the solutions to make the gain scheduling scheme practical, a saturation block with lower limit at 0 W and upper limit at 1 W is inserted after the controller. The simulation results with the saturation block is shown on Fig. 4. Since a similar performance is achieved with the saturation block, this gain scheduling scheme can be concluded as effective and practical.

Finally, we illustrate the worst case where nine out of ten channels are dropped. Even though glitches in the pump power, the total gain and the output channels are noticeable during the scheduling process from Fig. 5, the overall process is able to stabilize itself within 1 ms as specified. The settling time of the system is faster during channel dropping than that during channel adding. This is because we have normalized the closed loop system with respect to ω_{OL} of the plant. Since the magnitude of ω_{OL} is smaller with less input power, the system responds more slowly compared with the system with greater input power. Note that only the change in input power is simulated here. The change in the desired total gain can also be simulated with the same scheduling scheme and shown to have satisfactory results.

V. Conclusion and Future Directions

The total gain control of the EDFA by means of pump compensation in a WDM network is extensively explored. In this paper, we demonstrate that a gain scheduled simple PID controller manages to clamp the total gain of the EDFA with a settling time less than 1 ms. As the result, the output power of each channel stays relatively constant. This control scheme is effective over a wide range of operation considered in this paper. Our design takes into account of the practical issues such as accessible parameters and pump power limitation. Therefore, this gain scheduled controller is both economical and effective for real-life application.

As demonstrated in this paper, the controller design is greatly limited by the design constraints specific to EDFA's. There are only limited number of accessible parameters. If the state of the EDFA (i.e. the average upper level fraction) is measurable, more advanced design techniques such as state feedback, optimal control can be implemented. Therefore, one of the potential research objectives is to investigate nonlinear controllers for the case where the average upper level fraction is measurable.

References

[1] E. Desurvire, B. D. D. Bayart, and S. Bigo, *Erbium-Doped Fiber Amplifiers Device and System Developments*. New York: John Wiley and Sons, 2002.

[2] J. L. Zyskind, A. K. Srivastave, Y. Sum, J. C. Ellson, G. W. Newsome, R. W. Tkach, A. R. Chraplyvy, J. W. Sulhoff, T. A. Strasser, J. R. Pedrazzani, and C. Wolf, "Fast-link control protection of surviving channels in multiwavelength optical networks," *IEEE Photon. Technol. Lett.*, vol. 9, pp. 1667–1669, Dec. 1997.

[3] B. Clesca, V. Havard, S. Gauchard, V. Rodrigues, E. Lantonien, D. Cravec, and F. X. Ollivier, "Upper limit and control scheme for power per channel in optically-amplified WDM systems," in *Proc. ECOC's96*, vol. 9, 1996, pp. 333–336.

[4] L. Pavel, "Control design for transient power and spectral control in optical communication networks," in *Proc. IEEE Conference on Control Applications*, vol. 1, June 2003, pp. 415 – 422.

[5] L. Tančevski, L. A. Rusch, and A. Bononi, "Gain control in EDFA's by pump compensation," *IEEE Photon. Technol. Lett.*, vol. 10, no. 9, pp. 1313–1315, Sept. 1998.

[6] S. Y. Park, K. K. Kim, G. Y. Lue, S. M. Kang, and S. Shin, "Dynamic gain and output power control in gain-flattened erbium-doped fiber amplifier," *IEEE Photon. Technol. Lett.*, vol. 10, no. 6, pp. 787–789, June 1998.

[7] K. Motoshima, N. Suzuki, and K. Shimizu, "A channel-number insensitive erbium-doped fiber amplifier with automatic gain and power regulation function," *J. Lightwave Technol.*, vol. 19, no. 11, pp. 1759–1767, Nov. 2001.

[8] E. Desurvire, *Erbium-Doped Fiber Amplifier*. New York: John Wiley and Sons, 1994.

[9] Y. Sun, J. L. Zyskind, and A. K. Srivastava, "Average inversion level, modeling, and physics of erbium-doped fiber amplifiers," *IEEE J. Select. Topics Quantum Electron.*, vol. 3, pp. 991–1007, Aug. 1997.

[10] S. Skogestad and I. Postlethwaite, *Multivariable feedback control - analysis and control*. Toronto: John Wiley and Sons, 1996.

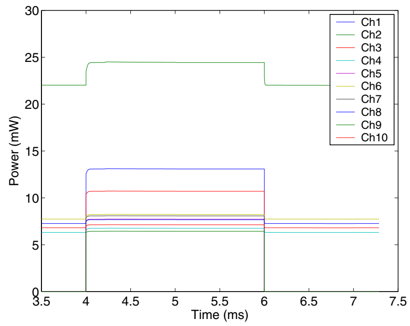

(a) p^{out} of the ten channels with the gain scheduled PID controller

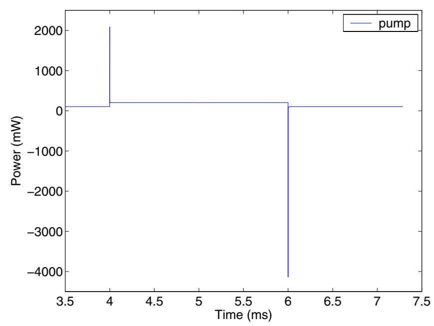

(b) p_{pump} with the gain scheduled PID controller

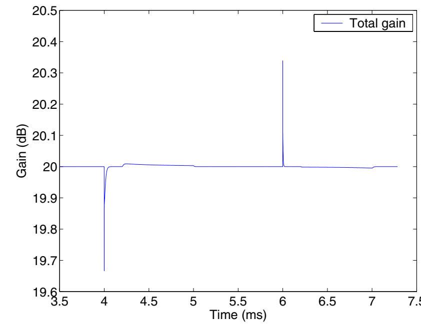

(c) total gain, G, with the gain scheduled PID controller

Fig. 3. System response with the scheduled PID controller and the nonlinear plant after five channels are added and dropped

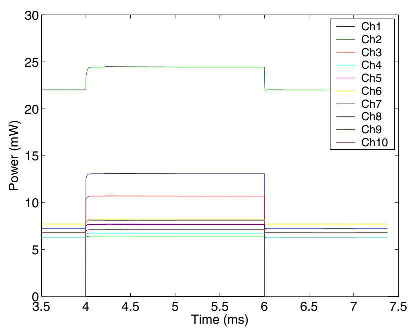

(a) p^{out} of the ten channels with the gain scheduled PID controller

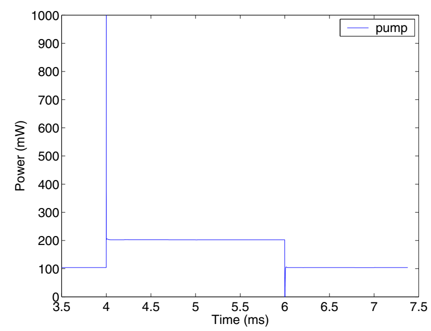

(b) p_{pump} with the gain scheduled PID controller

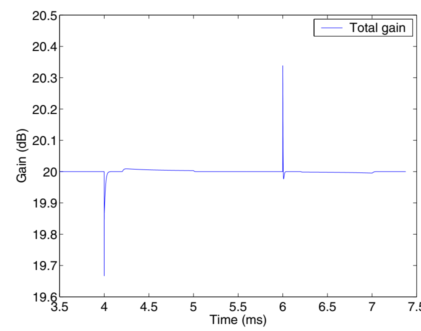

(c) total gain, G, with the gain scheduled PID controller

Fig. 4. System response with the PID controller, the nonlinear plant and the saturation block after five channels are added and dropped

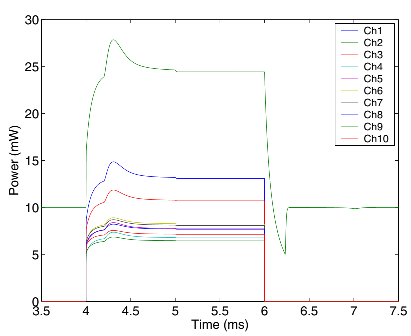

(a) p^{out} of the ten channels with the gain scheduled PID controller

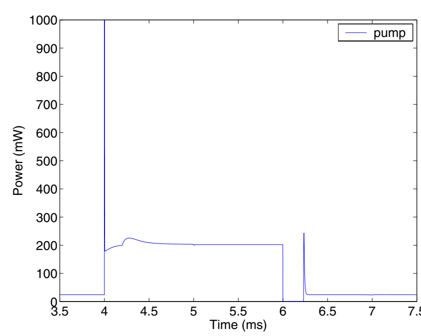

(b) p_{pump} with the gain scheduled PID controller

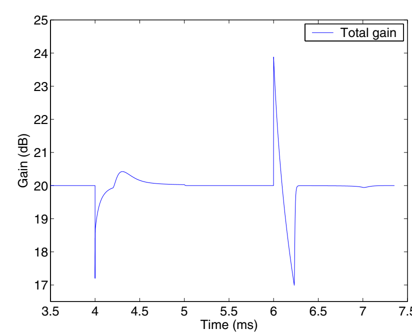

(c) total gain, G, with the gain scheduled PID controller

Fig. 5. System response with the PID controller, the nonlinear plant and the saturation block after nine channels are added and dropped

[11] L. S. William, *The Control Handbook*, ser. Electrical Engineering Handbook. Boca Raton: CRC Press, 1996, vol. 6.

[12] W. J. Rugh, "Analytical framework for gain scheduling," *IEEE Control Syst. Mag.*, vol. 11, pp. 79–84, Jan. 1991.

[13] R. A. Hyde and K. Glover, "The application of scheduled H-infinity controllers to a VSTOL aircraft," *IEEE Transactions of Automatic Control*, vol. 38, no. 7, pp. 1021–1039, 1993.

[14] R. A. Nichols, R. R. Reichert, and W. J. Rugh, "Gain scheduling for H-infinity controllers: A flight control example," *IEEE Trans. Automat. Contr.*, vol. 1, no. 2, pp. 69–75, June 1993.

[15] J. S. Shamma and M. Athans, "Gain scheduling: potential hazards and possible remedies," *IEEE Control Syst. Mag.*, vol. 12, no. 3, pp. 101–107, June 1992.

[16] J. Wang and W. J. Rugh, "On parameterized linear systems and linearization families for nonlinear systems," *IEEE Trans. Circuits Syst.*, vol. CAS-34, no. 6, pp. 650–657, 1987.

[17] D. J. Leith and W. E. Leithead, "Equivalence of gain-scheduling and input-output linearization for a class of commonly occurring plants," in *Proc. of the 36th IEEE Conference on Decision and Control*, vol. 1, Dec. 1997, pp. 430–431.